Research article

Relative wave energy-based adaptive neuro-fuzzy inference system for estimation of the depth of anaesthesia

V.K. Benzy[1,*], E.A. Jasmin[1], Rachel Cherian Koshy[2], Frank Amal[3], K.P. Indiradevi[1]

[1] *Department of Electrical Engineering, Govt. Engineering College, Thrissur, Kerala, India*
[2] *Department of Anaesthesiology, Regional Cancer Centre, Trivandrum, Kerala, India*
[3] *Department of Anaesthesiology, Railway Hospital, Palakkad, Kerala, India*

***Correspondence**: benzyvk@yahoo.com (V.K. Benzy)

https://doi.org/10.31083/JIN-170039

Abstract

Advances in medical research and intelligent modeling techniques have led to developments in anaesthesia management. The present study aims to estimate the depth of anaesthesia using cognitive signal processing and intelligent modeling techniques. The neurophysiological signal that reflects the cognitive state of anaesthetic drugs is the electroencephalogram signal. The information available from electroencephalogram signals during anaesthesia is extracted from the relative wave energy features of those signals. Discrete wavelet transform is used to decompose electroencephalogram signals into four levels and the relative wave energy is computed from approximate and detailed coefficients of the signal sub-bands. Relative wave energy is extracted to determine the degree of importance of different electroencephalogram frequency bands associated with different anaesthetic phases, for example, the awake, induction, maintenance, and recovery phases. The Kruskal–Wallis statistical test is applied to relative wave energy features to check the discriminative capability of the relative wave energy features classified as awake, light anaesthesia, moderate anaesthesia, and deep anaesthesia. A novel depth of anaesthesia index is generated by implementing an adaptive neuro-fuzzy inference system based on a fuzzy c-means clustering algorithm which uses relative wave energy features as inputs. Finally, the generated depth of anaesthesia index is compared with a commercially available depth of anaesthesia monitor, the Bispectral index.

Keywords

Electroencephalogram; relative wave energy; discrete wavelet; depth of anaesthesia; neurophysiological signal; adaptive neuro-fuzzy system

Submitted: May 14, 2017; **Accepted:** June 22, 2017

1. Introduction

General anaesthesia is a drug-induced reversible state that leads to loss of both consciousness and pain perception during surgical procedures. General anaesthetic drugs alter the responses of the central nervous system (CNS). Estimation of response during general anaesthesia depends upon variations in neurophysiological signals. During anaesthesia, these variations are reflected as amplitude and frequency variation of the electroencephalogram (EEG) waveform or signal [1]. Traditionally, the frequencies of an EEG signal were divided into five rhythms, gamma, alpha, beta, theta, and delta [2]. Analysis of EEG signals to explore cognitive states leads to the evolution of EEG-based anaesthesia monitors. The complexity of EEG signals as well as their high sensitivity to various types of artefacts, has prevented the development of anaesthetic monitoring. Most complications of anaesthesia involve patient awareness during surgery due to inadequate doses of anaesthetic drugs, with an excessive depth of anaesthesia leading to delayed recovery from anaesthesia. Therefore, continuous monitoring of anaesthesia should avoid inadequate levels of anaesthesia. Bispectral index scale (BIS), Auditory Evoked Potential (AEP), Narcotrend, Cerebral state Monitor, and Entropy are some of the commercially available depth of anaesthesia (DoA) monitors. The advantage of these monitors is that during surgery anaesthetist can tailor a dose of anaesthetic drugs administered to a patient. Among these monitors, the BIS monitor developed by Aspect Medical Systems in 1996 is a reliable comparison standard for DoA monitoring due to its usefulness and effectiveness.

The BIS monitor provides an index ranging from 0 to 100. Zero indicates a state of no brain activity and 100 indicates full wakefulness. The range 0–100 can be subdivided into five states. 0–20 is the burst suppression state, considered to be a very deep anaesthetic state. 20–40 is a deep anaesthetic state, 40–60 a moderate anaesthetic state, 60–80 a light anaesthetic state, and 80–100 is the awake state. The moderate anaesthetic state is considered to be an appropriate level for surgery under general anaesthesia [3].

The cognitive signal processing based on EEG signals for the monitoring of DoA was first observed by Zhang *et al.* [4]. It quantitatively analyzes the complexity of EEG signals using a Lempelziv complexity (LZC) algorithm. Gifani *et al.* [5] used detrended fluctuation analysis (DFA) to differentiate awake and anesthetized states. This was further demonstrated by Jospin *et al.* [6] and Kaplan *et al.* [7]. Fan *et al.* [8] and Ferenets *et al.* [9] adopted nonlinear methods to quantify EEG variations during anaesthesia. To overcome the difficulties of DFA in discriminating between wakefulness and deep

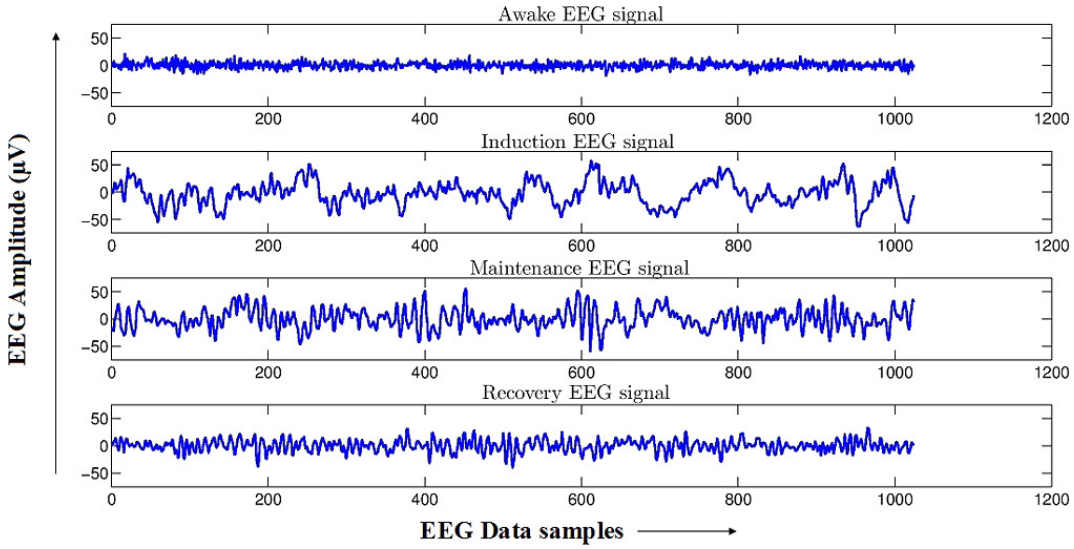

Fig. 1. Plot of one segment of EEG signal each corresponding to Awake, Induction, Maintenance, and Recovery phases of anaesthesia. Each segment represents eight seconds of EEG data or 1024 data points.

anaesthesia, Nguyen-Ky *et al.* [10] developed an improved detrended moving-average method, while Palendeng *et al.* [11] used the phase and amplitude of EEG signals as measures of DoA.

Earlier frequency analysis of EEG signals employed Fourier transform (FT) techniques. The drawback of FT is that the time component is lost in the frequency domain [12]. To overcome this difficulty, wavelet transform (WT) is used in the analysis of biomedical signals. Nguyen-Ky *et al.* [13] employed WT and an eigenvector to predict the unknown characteristics of anaesthetic related EEG signals. Zoughi *et al.* [3] found that a wavelet feature, the wavelet coefficient energy entropy (WCEE) varies with anaesthetic depth. The spectral edge frequency (SEF) feature extracted from EEG signals was previously used in sleep stage classification [14]. Otto *et al.* [15] extracted SEF from sheep EEG signals to measure DoA.

Most medical research applications employ intelligent techniques for estimation and classification of different physiological signals [16–18]. The intelligent modeling of DoA monitoring incorporates features extracted from the EEG as input to an artificial neural network (ANN), fuzzy inference systems, and hybrid systems. Classification of DoA using ANN and EEG extracted permutation entropy was done by Shalbaf *et al.* [19]. The computation of permutation entropy (PE) is efficient in EEG analysis, but fails to work for deep anaesthetic states[20]. Esmaeili *et al.* [21] developed a fuzzy rule-based system that integrated EEG features for estimation of DoA.

2. Methodology

2.1. Data acquisition

The data used for the present analysis were obtained from 25 female subjects in the age range 30–78 years who had undergone breast cancer surgery under general anaesthesia at Regional Cancer Centre, Trivandrum, Kerala, India. A written informed consent was obtained from all participating subjects and the study protocol was approved by the institutional medical ethical committee.

Each subject was pre-medicated with Alprazolam (0.25 to 0.5 mg), Pantoprazole (40 mg), and Domperidone (10 mg) at 10 PM the night before surgery and at 6 AM on the day of surgery. An intravenous line was started just before surgery and Glycopyrolate (0.2 mg), Midazolam (1 mg), and Fentanyl 1 μg/kg were given just prior to the start of surgery. Additionally, analgesic drugs like Paracetamol (1 g), Diclofenac sodium (75 mg), an intravenous anaesthetic drug propofol (2 mg/kg), and a muscle relaxant drug Vecuronium Bromide (0.1 mg/kg) were given during the surgery. TPatients were ventilated with oxygen (O_2)-Sevoflurane and nitrous oxide (N_2O) to maintain anaesthesia for the duration of the surgery. Additional doses of Fentanyl, up to 0.5 μg/kg, were given if blood pressure (BP) or heart rate (HR) increased more than 20 percent above base line. If the BP or HR was not controlled by Fentanyl then Nitroglycerin (NTG) was administered to control BP and Metoprolol was used to control HR.

A BIS electrode was used to collect the EEG signal and BIS value from each subject. The EEG signal was sampled at 128 samples per sec. The collected EEG database was classified as awake, induction, maintenance, and recovery signal depending upon the time at which data was collected [22].

(i) Awake signal: EEG signals collected 5–10 minutes before administering intravenous anaesthetic agents. Corresponding BIS values ranged between 80–100.
(ii) Induction signal: EEG signals collected from administration time of intravenous anaesthetic agents to absence of response to verbal stimuli (checked by anesthetist). Corresponding BIS values ranged between 20–40.
(iii) Maintenance signal: EEG signals collected after insertion of endotracheal tube and administration of inhalation agent until the end of surgery. Corresponding BIS value ranged between 40–60.
(iv) Recovery signal: EEG signals collected after the cut off of inhalation agent and administration of reversal agent (Neostigmine and Glycopyrolate) until return of consciousness. Corresponding BIS values ranged between 60–80.

EEG signals corresponding to BIS values of 0–20 were not analyzed due to the possibility of hemodynamic instability of the

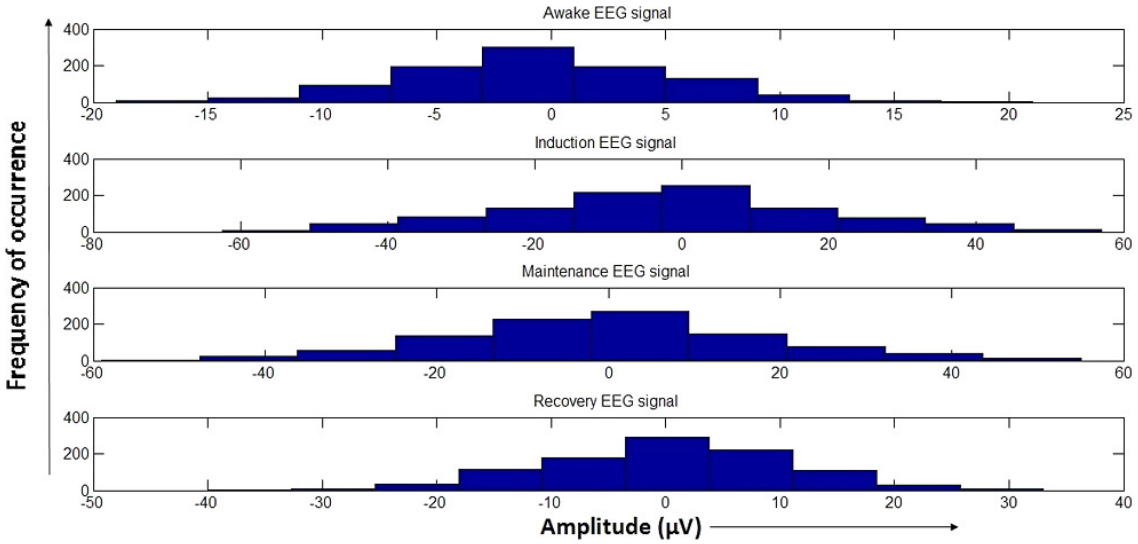

Fig. 2. Histogram of EEG signals corresponding to different phases of subject anaesthesia. Amplitude range of awake EEG signal was −15 to +15 μV, induction signal −50 to +50 μV, maintenance signals −40 to +40 μV, and recovery signal −25 to +25 μV.

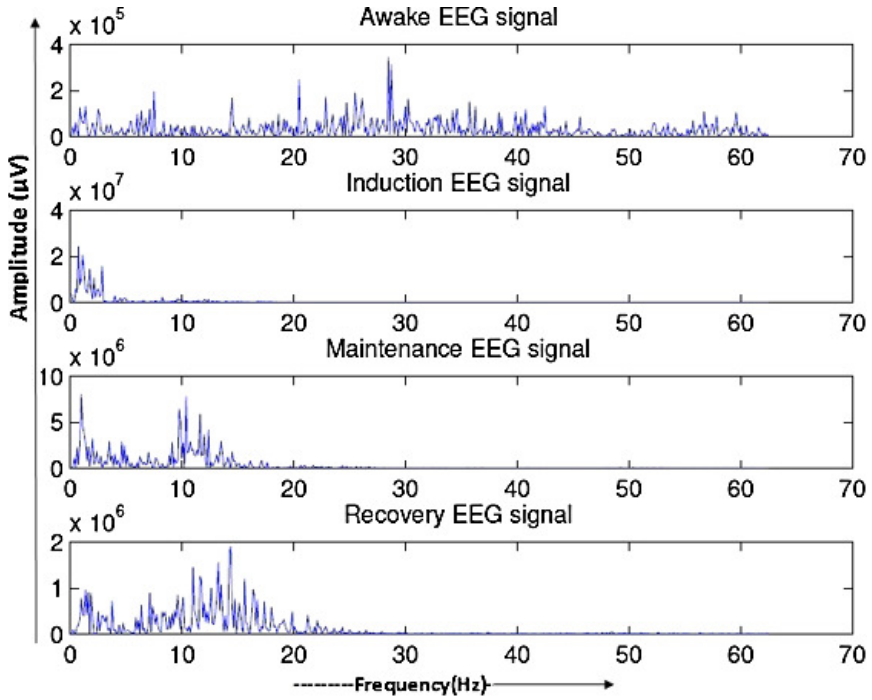

Fig. 3. EEG signal frequency spectrum corresponding to different phases of anaesthesia. Frequency range of awake EEG signal 0–60 Hz, induction signal 0–5 Hz, maintenance signals 0–20 Hz, and recovery signal 0–30 Hz.

patient during surgery and hence were beyond the scope of this study.

2.2. *Preprocessing and segmentation*

A 50 Hz notch filter was used to remove power line interference from the recorded EEG signals [3]. EEG signals were segmented using a uniform segmentation method that divides EEG signals into non-overlapping rectangular windows of eight second duration [23]. Fig. 1 shows one segment of EEG signal corresponding to each different phase of anaesthesia. Amplitude of the EEG signal increases and frequency decreases with increase in DoA. Induction EEG signals are deep, maintenance EEG signals are moderate, and recovery EEG signals are light anaesthetic EEG signals. One segment of EEG signal was eight seconds of data or 1024 data samples.

The time and frequency distribution of the awake, induction, maintenance, and recovery EEG signals were analyzed using histograms and frequency distribution plots. Plots in Fig. 2 shows the histogram and Fig. 3 shows the frequency spectrum corresponding to an eight second EEG recording of a subject in each phase. The amplitude of the EEG signal increases and the frequency decreases when the DoA increases [24]. Amplitude variations were more vis-

ible in the histogram. For awake EEG signals the amplitude range was −15 to +15 μV, induction signal (very deep anaesthetic) range was −50 to +50 μV, maintenance signal (deep anaesthetic) range was −40 to +40 μV, and for recovery signal (light anaesthetic) the amplitude ranged from −25 to +25 μV. It is clear from the frequency spectrum shown in Fig. 3 that frequency reduced when anaesthesia depth increased. The frequency spectrum EEG signals of the deep anaesthesia state (induction phase) contained lower frequency components, whereas, the awake EEG signal contained higher frequency components [22].

2.3. *Feature extraction*

The major challenges for EEG based analysis of DoA are the inherent non-stationarities and complexity of the data. If surgery has a three hour duration, then the EEG data for a single subject consists of more than 13 lakh of data points (10800 second data duration). Analyzing all these data points is time consuming. Therefore, the EEG signal dimensionality was reduced by extracting the RWE. The extracted RWE feature discriminated the different anaesthetic states, awake, light anaesthesia, moderate anaesthesia, and deep anaesthesia.

2.3.1. Relative Wavelet Energy

The time-frequency representation of a signal can be done effectively obtained by wavelet transform (WT). At low frequencies, a WT gives a lower temporal resolution and high frequency resolution, whereas, at high frequencies it gives a high temporal resolution and lower frequency resolution [22]. Most biomedical signals are non-stationary, thus a WT is best suited for locating transient events. The present study employed wavelet based feature extraction and multiresolution analysis to analyze the various transient events in the EEG of awake and anaesthetized subjects. Multiresolution analysis decomposes EEG signals into a number of frequency bands. Discrete wavelet transform (DWT) with Mallat's fast algorithm is commonly used for EEG signal analysis [25].

The RWE feature extraction algorithm is described by [22, 26]:

(1) Decomposition of EEG signals into detail and approximation coefficients using DWT is given by

$$cA_j(n) = \sum g(l-2n)cA_{j-1}(l) \tag{1}$$

$$cD_j(n) = \sum h(l-2n)cD_{j-1}(l) \tag{2}$$

Here $cD_j(n)$ and $cA_j(n)$ give the detail and approximation coefficients of an EEG signal and g and h provide low and high pass filters for the EEG signals.

(2) Calculation of wavelet coefficient total energy

$$E_{m,\text{total}} = \sum_{j=1}^{4}\sum_{k=1}^{m}|cD_j(k)|^2 = \sum_j E_{m,j} \tag{3}$$

where m is the window length of the EEG segment, j is the level of decomposition and $E_{m,j}$ is the energy of the kth sample is given by

$$E_{m,j} = \sum_{j=1}^{4}|cD_j(k)|^2 \tag{4}$$

(3) Relative wavelet energy is obtained from

$$\rho_{m,j} = \frac{E_{m,j}}{E_{m,\text{total}}} \tag{5}$$

The goals of wavelet based RWE feature extraction are (i) decompose EEG signals into their constituent frequency bands, (ii) provide the concept of RWE associated with EEG frequency bands, and (iii) determine the degree of importance of different frequency bands during the different anaesthetic phases.

2.4. *Statistical analysis*

The Kruskal–Wallis statistical test was employed to determine whether the extracted RWE features discriminate the different anaesthetic levels as awake, light anaesthesia, moderate anaesthesia, and deep anaesthesia.

2.4.1. Kruskal–Wallis test

The Kruskal–Wallis test or one-way ANOVA on ranks is a non-parametric method for testing whether samples originate from the same distribution [27, 28]. It is employed to determine the statistically significant differences between two or more groups of an independent variable and a continuous or ordinaly dependent variable. The test determines whether the groups are statistically different or not.

2.5. *Adaptive neuro-fuzzy inference system (ANFIS)*

An adaptive neuro-fuzzy inference system artificial neural network based on the Takagi–Sugeno fuzzy inference system was employed. ANFIS integrates neural network and fuzzy logic principles and has the potential to capture the benefits of both paradigms in a single system. Its inference system consists of a set of fuzzy IF-THEN rules and has the ability to approximate nonlinear functions [29]. In ANFIS, membership function parameters are extracted from the data set that describes system behavior. The ANFIS learns features from the data set and adjusts system parameters according to an error criterion [30]. In the present study ANFIS utilizes a fuzzy c-means (FCM) clustering method to learn and adjust its parameters. In this clustering algorithm, introduced by Bezdek *et al.* [31], each data point belongs to a cluster to a degree specified by the membership grade.

3. Results and discussions

3.1. *Feature extraction*

RWE features measure DoA based on relative energy across its frequency bands and varyies with the transformation in depth of anaesthesia. EEG signals corresponding to the BIS value range of 0–20 were not obtained during surgery for reasons of patient safety and hence were not analyzed.

3.1.1. Relative Wave Energy (RWE)

Awake and anaesthetised EEG signals were decomposed into the frequency ranges delta, theta, alpha, beta, and gamma using multiresolution analysis by WT. RWE was then extracted from the required frequency ranges for each subject. DWT with a Doubechies-4 mother wavelet was used for the decomposition and the decomposition level was four. The decomposition of the EEG signal into its frequency bands was obtained by successive convolution with high-pass and low-pass filtering of the signal. The low frequency components were obtained from the approximation coefficients and high frequency components from the detail coefficients. Fig. 4 shows the four-level

decomposition of EEG signals with a sampling frequency of 128 Hz. CA1, CA2, CA3, and CA4 are the approximation coefficients and CD1, CD2, CD3, and CD4 are the detail coefficients obtained after successive decomposition. Frequency bands corresponding to four-level decomposition of EEG signals are shown in Table 1. The sub-band frequencies obtained from the DWT coefficients of the awake EEG signal of a subject and its four detail (CD1–CD4) and approximate (CA4) frequency band signals are shown in Fig. 5. The relative wave energies RWE1, RWE2, RWE3, RWE4, and RWE5 are computed using energies of the CD1 to CD4 and CA4 frequency band signals. Similarly, the RWE1, RWE2, RWE3, RWE4, and RWE5 features were computed from induction, maintenance, and recovery EEG signals and their DWT decomposition. RWE feature extracted from a single segment of EEG signal from four anaesthetic phases of a subject are shown in Table 2.

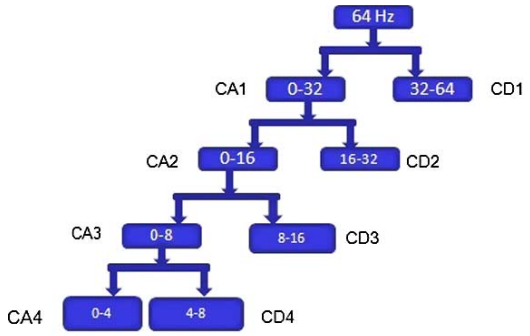

Fig. 4. Wavelet based decomposition of EEG signals into different frequency bands. CA1, CA2, CA3, and CA4 represent the approximation coefficients and CD1, CD2, CD3, and CD4 represent the detail coefficients of the wavelet decomposition.

Table 1. Frequency Bands and Decomposition

Frequency Range	Frequency Bands	Decomposition levels	Frequency Bandwidth
Gamma	32–64	cD1	32
Beta	16–32	cD2	16
Alpha	8–16	cD3	8
Theta	4–8	cD4	4
Delta	0–4	cA4	4

Table 2. RWE variations during different anaesthetic phases

Frequency Range (Hz)	RWE	Awake	Induction	Maintenance	Recovery
32–64	RWE1	0.4408	0.0127	0.015	0.1775
16–32	RWE2	0.1226	0.0492	0.0706	0.182
8–16	RWE3	0.1985	0.107	0.2028	0.2262
4–8	RWE4	0.0868	0.2826	0.3289	0.144
0–4	RWE5	0.0713	0.7485	0.382	0.0694

From the Table 2 it is clear that the values of RWE1 are high in the awake phase because when a subject is awake high frequency components will be more active due to anxiety and stress. However, when anaesthetized, the RWE values of low frequency components become active. Therefore, during the deep anaesthetic state (induction phase) RWE5 is high. In the maintenance phase RWE values of theta and delta, i.e. RWE4 and RWE5, show almost similar values and in recovery phase, RWE values of the alpha band (RWE3) are active compared to the other bands.

The RWE distribution of a subject during six continuous segments of different anaesthetic phases are shown in Fig. 6. It can be seen from the figure that during the awake phase RWE values of gamma, beta, and alpha frequency bands are high, which is usually seen in the conscious state. During induction the patient loses consciousness and the RWE values of delta and theta increase with prominent delta activity values. There are decreased RWE values for alpha, beta, and gamma activity. Also seen are the waxing and waning effects of the RWE values of alpha, theta, and delta. In the maintenance phase the inhalational agent sevoflurane induces the predominant RWE values of theta and delta activity with reduced RWE values for alpha, beta, and gamma. During recovery, sevoflurane is curtailed and the subject starts to regain consciousness after the effects of the anaesthetic drugs. Thus, there is a sudden increase in the RWE values of alpha, beta, and gamma activity, with prominent alpha activity.

3.1.2. Statistical analysis

The discriminative ability of the features RWE1–RWE5 extracted from all 25 subjects during the entire surgery was tested by application of the Kruskal–Wallis statistical test to the features RWE1–RWE5. The output groups for the discrimination are Awake, Light Anaesthesia, Moderate Anaesthesia, and Deep Anaesthesia which is the anaesthetic depth given for each subject by the attending anaesthetist. The p-values obtained from the Kruskal–Wallis tests are given in Table 3. The highest p-values are for the feature RWE4 and RWE3 which indicates that RWE4 and RWE3 had the lowest discriminative ability when compared to other features. On the other hand RWE1, RWE2, and RWE5 had the highest discriminative ability. The features RWE4 and RWE3 were eliminated from further processing because of their poor discriminative ability. Box plots of the features RWE1–RWE5 during different anaesthetic depths are shown in Fig. 7a–7e. From the box plots it is clear that the RWE values of RWE1 and RWE2 are inversely proportional to the depth of anaesthesia, as it increases the RWE values decrease. On the other hand, RWE5 shows a direct relation to anaesthetic depth and their values increase with increased in depth.

3.2. Adaptive neuro-fuzzy inference system

An adaptive neuro-fuzzy inference system was implemented to generate an index that continuously measured the anaesthetic depth based on extracted RWE features. The features RWE1, RWE2, and RWE5 were given as inputs to the neuro-fuzzy system. This study utilized an ANFIS-Fuzzy c-means clustering method to generate the DoA index. In conventional fuzzy inference systems the membership functions and the rules are decided by experts who have a thorough knowledge about the inputs and outputs. In the present ANFIS-FCM model, membership functions (MFs) and rules were realized by training a data set of input-output pairs. However, the number of MFs were assigned empirically [32, 33].

The architecture of the ANFIS-FCM model for the estimation of DoA is shown in Fig. 8. The data sets for training and validation incorporated the extracted features RWE1, RWE2, and RWE5 from the EEG signals of 25 patients consisting of 17,935 3-D vectors.

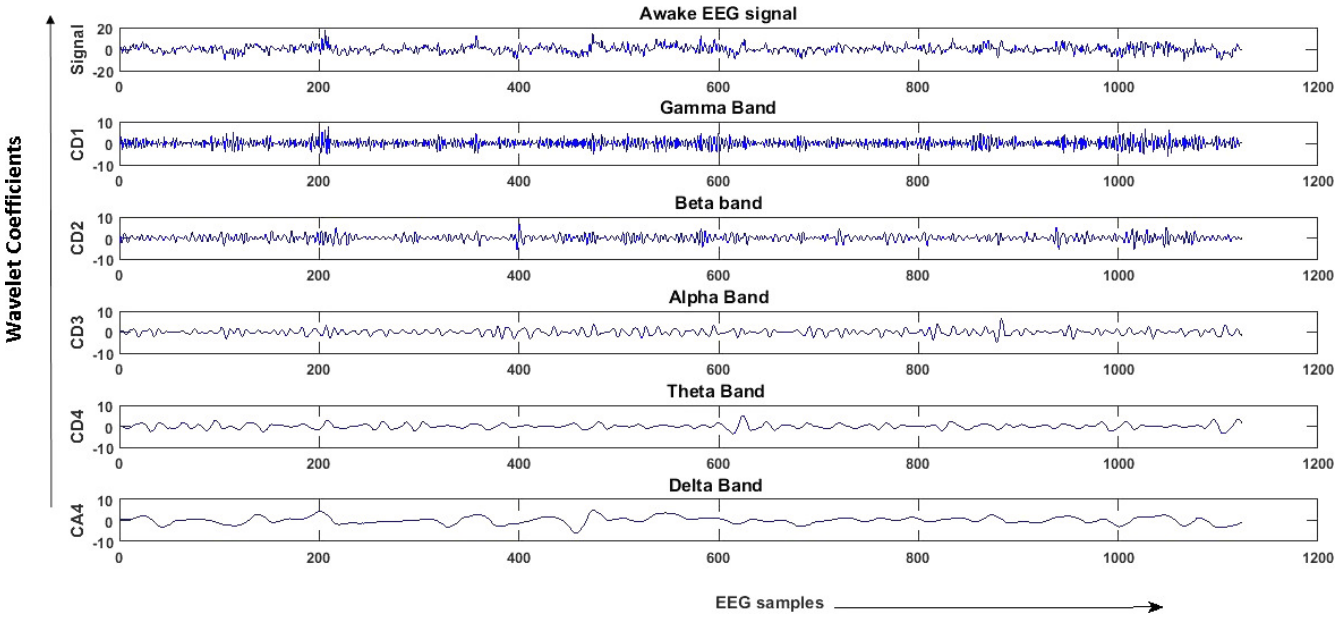

Fig. 5. Wavelet decomposition of EEG signals corresponding to the awake phase is shown where CA4, CD4, CD3, CD2, and CD1 represent the frequency bands of Delta, Theta, Alpha, Beta, and Gamma respectively.

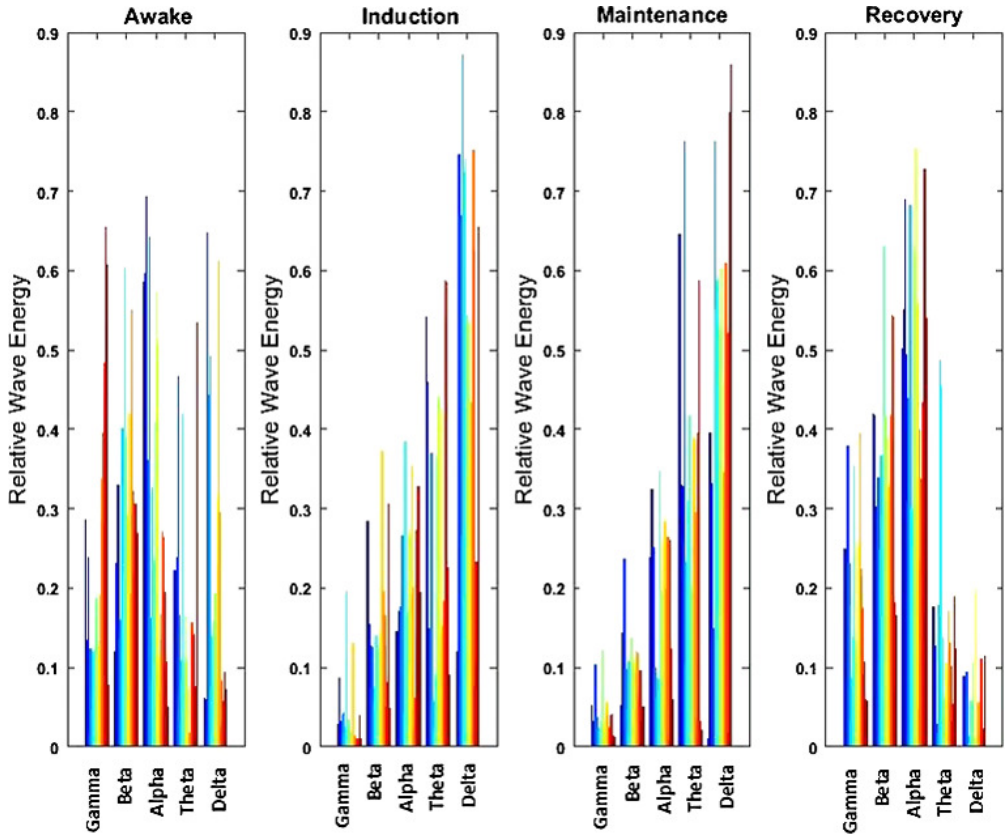

Fig. 6. Comparison of relative wavelet energy during the four phases of anaesthesia studied. Each figure shows the strength of the EEG frequency bands corresponding to awake, induction, maintenance, and recovery signals.

13,166 3-D vectors were utilized for construction of the model by training, and the remaining 4,373 3-D vectors were used for evaluating the performance of the ANFIS-FCM model that was developed. Fig. 9 shows the membership functions of the input parameters RWE1, RWE2, and RWE5 and Table 4 shows the specification of the ANFIS-FCM model. This model was implemented to generate

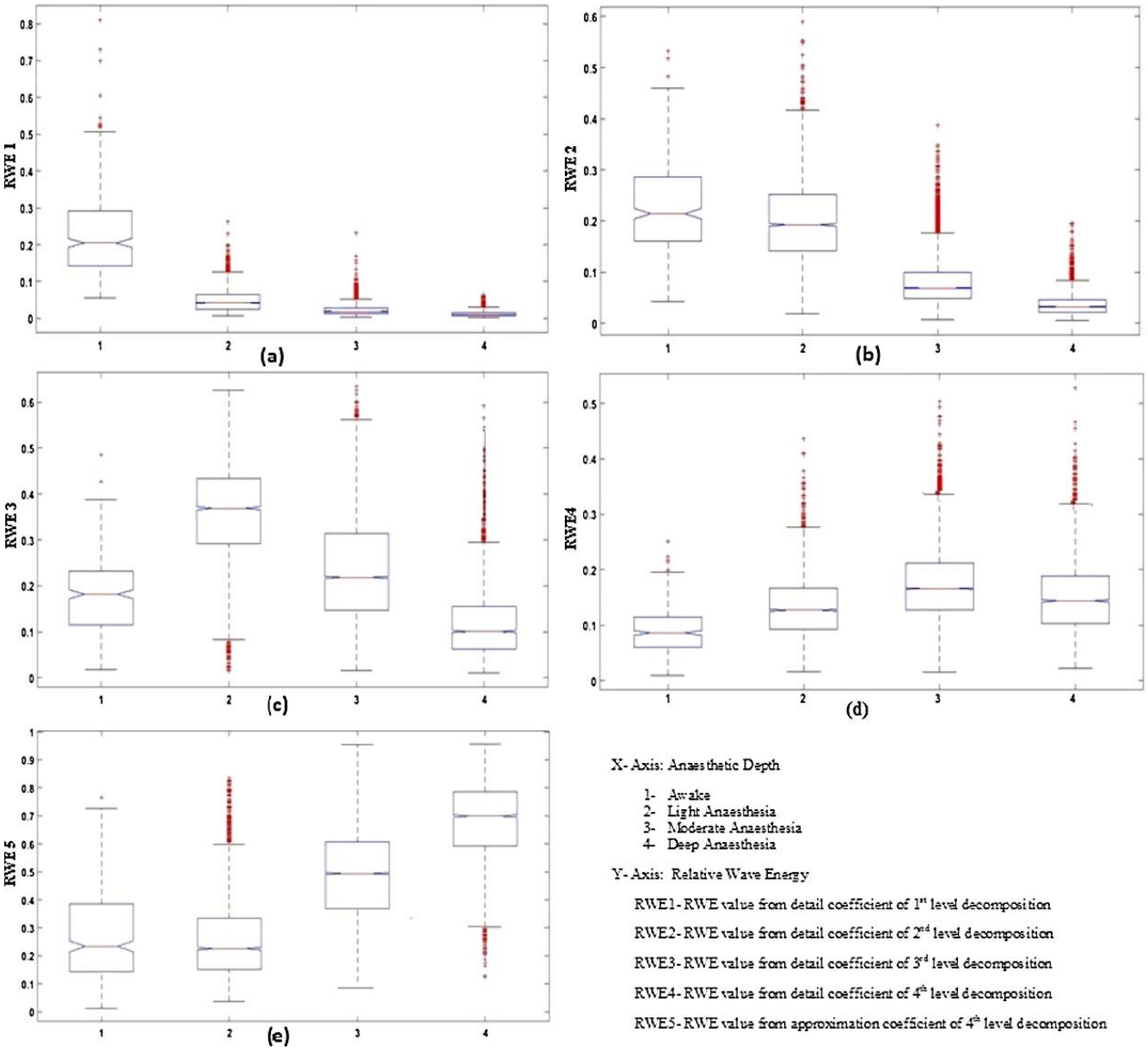

Fig. 7. Box plot of RWE1-RWE5 computed from the decomposition coefficients of EEG signals. 1, 2, 3, and 4 in the *X*-axis represent the output groups awake, light anaesthesia, moderate anaesthesia, and deep anaesthesia.

Table 3. *p*-value of the features RWE1–RWE5 obtained from a Kruskal–Wallis statistical test

	RWE1	RWE2	RWE3	RWE4	RWE5
p-value	3.27×10^{-8}	4.84×10^{-6}	1.93×10^{-3}	7.40×10^{-2}	1.46×10^{-4}

a dimensionless index ranging from 0 to 100 similar to a BIS index where 0 indicates no brain activity and 100 indicates the fully awake state. The RWE and ANFIS-FCM based DoA index of patient-12 is shown in Fig. 10.

The Pearson correlation between the proposed DoA index and the BIS index for the particular patient is 81.6%. The average Pearson correlation obtained for all 25 patients is 79.7%.

4. Conclusion

The present study extracts RWE features of EEG signals recorded during different phases of anaesthesia. The RWE feature were extracted by decomposing the EEG signals into their constituent frequency components and then the relative energy of each frequency component was computed. It was found that the RWE features of the awake phase were high for high frequency bands and RWE values of the low frequency bands became high when subjects were

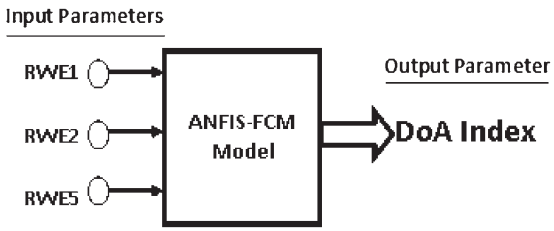

Fig. 8. Architecture of ANFIS-FCM model. RWE1, RWE2, and RWE5 are the inputs to the ANFIS-FCM model and the DoA index is the model outcome.

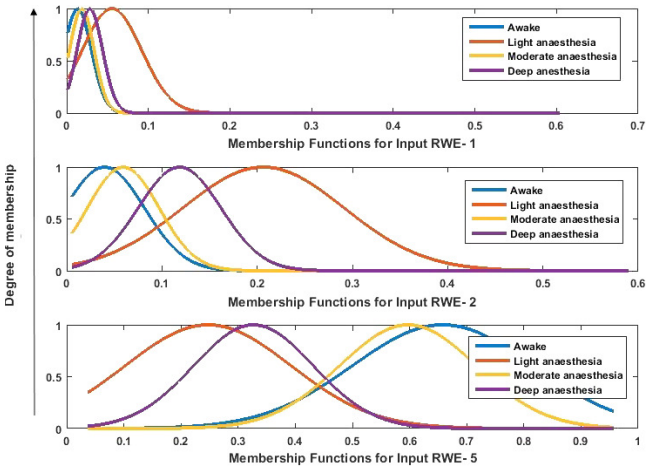

Fig. 9. Membership functions corresponding to different anaesthetic outcomes Awake, Light anaesthesia, Moderate anaesthesia, and Deep anaesthesia of the inputs RWE1, RWE2, and RWE5 extracted from the ANFIS-FCM Model.

Table 4. Specification of ANFIS-FCM Model

Specification	Description
Input Membership Function	Gaussian
Output Membership Function	Linear
Number of nodes	56
Number of linear parameters	24
Number of nonlinear parameters	40
Total number of parameters	64
Number of training data pairs	13166
Number of checking data pairs	4373
Number of fuzzy rules	4

anaesthetized. The discrimination ability of the extracted RWE features as Awake, Light Anaesthesia, Moderate Anaesthesia, and Deep Anaesthesia, were tested by applying a Kruskal–Wallis statistical test. RWE1, RWE2, and RWE5 showed high discriminativeability and RWE3 and RWE4 were eliminated from further processing. Finally, an ANFIS-FCM model was implemented using RWE1, RWE2, and RWE5 features to generate a novel and intelligent DoA index that varied according to the depth of anaesthesia. The study shows that it is easy to compute the DoA index and assist the anaesthetist in accurate and intelligent decision making. It also helps in the management of drug dose when used in real time and prevents patient awareness during surgery.

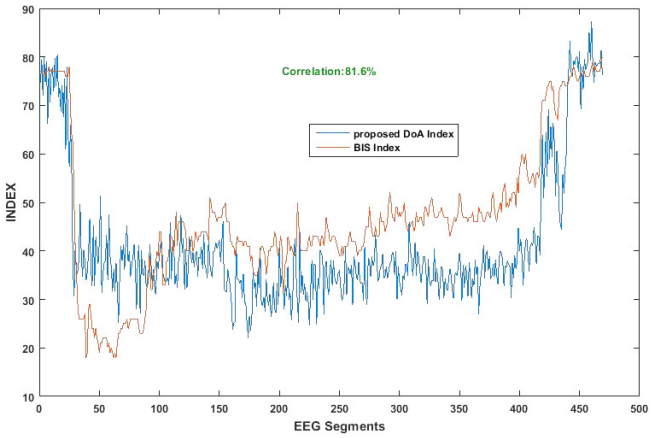

Fig. 10. Comparison of proposed DoA index with BIS. The Pearson correlation between the proposed DoA index and the BIS index of this particular patient throughout the surgery was 81.6%.

Acknowledgments

The authors would like to thank the members of anaesthesia team of Regional Cancer Center, Trivandrum for providing facilities for data collection and their knowledge and expertise in anesthesia management.

Conflict of Interest

All authors declare no conflicts of interest.

References

[1] Voss L, Sleigh J (2007) Monitoring consciousness: the current status of EEG-based depth of anaesthesia monitors. *Best Practice & Research Clinical Anaesthesiology* **21(3)**, 313-325.

[2] Alkadi M, Reaz MBI, Mohd Ali M (2013) Evolution of Electroencephalogram Signal Analysis Techniques during Anesthesia. *Sensors* **13(5)**, 6605-6635.

[3] Zou GT, Boostani R, Deypir M (2012) A wavelet-based estimating depth of anesthesia. *Engineering Applications of Artificial Intelligence* **25(8)**, 1710-1722.

[4] Zhang XS, Roy RJ, Jensen EW (2001) EEG complexity as a measure of depth of anesthesia for patients. *IEEE Transactions on Biomedical Engineering* **48(12)**, 1424-1433.

[5] Gifani P, Rabiee H, Hashemi Golpayegani SMR, Ghanbari M (2005) Extraction of anesthesia depth using self similarity and fluctuation analysis on the wavelet coefficients of EEG. In, The 3rd IEE International Seminar on Medical Applications of Signal Processing (Ref. No. 2005-1119), London, UK.

[6] Jospin M, Caminal P, Jensen E, Litvan H, Vallverdu M, Struys M, Vereecke H, T Kaplan D (2007) Detrended Fluctuation Analysis of EEG as a Measure of Depth of Anesthesia. *IEEE Transactions on Biomedical Engineering* **54(5)**, 840-846.

[7] Kaplan D (2006) Detrended Fluctuation Analysis of EEG as a Measure of Depth of Anesthesia. *IEEE Transactions on Biomedical Engineering* **53(11)**, 840-846.

[8] Fan SZ, Yeh JR, Chen BC, Shieh JS (2011) Comparison of EEG Approximate Entropy and Complexity Measures of Depth of Anaesthe-

sia During Inhalational General Anaesthesia. *Journal of Medical & Biological Engineering* **31(5)**, 359-366.

[9] Ferenets R, Lipping T, Anier A, Jäntti V, Melto S, and Hovilehto S (2006) Comparison of Entropy and Complexity Measures for the Assessment of Depth of Sedation. *IEEE Transactions on Biomedical Engineering* **53(6)**, 1067-1077.

[10] Nguyen-Ky T, Wen P, Li Y (2010) An Improved Detrended Moving-Average Method for Monitoring the Depth of Anesthesia. *IEEE Transactions on Biomedical Engineering* **57(10)**, 2369-2378.

[11] Palendeng ME, Wen P, Li Y (2014) Real-time depth of anaesthesia assessment using strong analytical signal transform technique. *Australasian Physical & Engineering Sciences in Medicine* **37(4)**, 723-730.

[12] Yong YPA, Hurley NJ, Silvestre GCM (2005) Single-trial EEG classification for brain-computer interface using wavelet decomposition. In, 13th European Signal Processing Conference (pp. 1-4) IEEE.

[13] Nguyen-Ky T, Wen P, Li Y, Malan M (2012) Measuring the hypnotic depth of anaesthesia based on the EEG signal using combined wavelet transform, eigenvector and normalisation techniques. *Computers in Biology and Medicine* **42(6)**, 680-691.

[14] Fell J, Röschke J, Mann K, Schäffner C (1996) Discrimination of sleep stages: A comparison between spectral and nonlinear EEG measures. *Electroencephalography and Clinical Neurophysiology* **98(5)**, 401-410.

[15] Otto KA, Cebotari S, Höffler HK, Tudorache I (2012) Electroencephalographic Narcotrend index, spectral edge frequency and median power frequency as guide to anaesthetic depth for cardiac surgery in laboratory sheep. *The Veterinary Journal* **191(3)**, 354-359.

[16] Yuvaraj R, Murugappan M, Ibrahim NM, Omar MI, Sundaraj K, Mohamad K, Palaniappan R, Satiyan M (2014) Emotion classification in Parkinson's disease by higher-order spectra and power spectrum features using EEG signals: a comparative study. *Journal of Integrative Neuroscience* **13(1)**, 89-120.

[17] Nguyen T, Khosravi A, Creighton D, Nahavandi S (2015) EEG signal classification for BCI applications by wavelets and interval type-2 fuzzy logic systems. *Expert Systems with Applications* **42(9)**, 4370-4380.

[18] Übeyli ED (2009) Combined neural network model employing wavelet coefficients for EEG signals classification. *Digital Signal Processing* **19(2)**, 297-308.

[19] Shalbaf R, Behnam H, Sleigh JW, Steyn-Ross A, Voss LJ (2013) Monitoring the depth of anesthesia using entropy features and an artificial neural network. *Journal of Neuroscience Methods* **218(1)**, 17-24.

[20] Shalbaf R, Behnam H, Jelveh Moghadam H (2015) Monitoring depth of anesthesia using combination of EEG measure and hemodynamic variables. *Cognitive Neurodynamics* **9(1)**, 41-51.

[21] Esmaeili V, Assareh A, Shamsollahi M, Moradi M, M. Arefian N (2008) Estimating the depth of anesthesia using fuzzy soft computation applied to EEG features. *Intelligent Data Analysis* **12(4)**, 393-407.

[22] Benzy Vk, Jasmin EA, Koshy R, Amal F (2016) Wavelet Entropy as a measure of Depth of Anaesthesia. In, Signal Processing and Integrated Networks, 3rd International Conference on (pp. 616-619) IEEE.

[23] Motamedi-Fakhr S, Moshrefi-Torbati M, Hill M, Hill CM, White PR (2014) Signal processing techniques applied to human sleep EEG signals—A review. *Biomedical Signal Processing & Control* **10(2)**, 21-33.

[24] Kelley SD (2003) *Monitoring level of consciousness during anesthesia and sedation*. Newton, MA, Aspect Medical Systems, Inc.

[25] Mallat GS (1998) *A Wavelet Tour of Signal Processing: The Sparse Way*. Orlando, FL., Academic Press.

[26] Benzy Vk, Jasmin EA, Koshy R, Amal F (2016) Wavelet Entropy based classification of depth of anesthesia. In, Computational Techniques in Information and Communication Technologies (ICCTICT), 2016 International Conference on (pp. 521-524),IEEE.

[27] Daniel WW (1990) Kruskal-Wallis one-way analysis of variance by ranks. In, WW Daniel (eds.) *Applied Nonparametric Statistics* (pp. 226-230), Boston, PWS-Kent.

[28] Statistics L (2013) *Kruskal-Wallis H test using SPSS*. Acedido em agosto, Lund Research Ltd.

[29] Abraham A (2005) Adaptation of Fuzzy Inference System Using Neural Learning. In, N Nedjah, LDM Mourelle (Eds.) *Fuzzy Systems Engineering* (pp. 53-83) Berlin, Heidelberg, Springer.

[30] Jang JS (1993) ANFIS Adaptive-Network-based Fuzzy Inference System. *IEEE Transactions on Systems, Man, and Cybernetics* **23(3)**, 665-685.

[31] Bezdek JC (1973) Fuzzy mathematics in pattern classification. PhD Thesis, Applied Math Center, Cornell University.

[32] Turksen B, Bilgiç T (2000) Measurement of membership functions: Theoretical and empirical work. In, D Dubois, H Prade (Eds.) *Fundamentals of Fuzzy Sets* (pp. 195-227), Boston, Springer.

[33] Abbod MF, Mahfouf M, Linkens DA (2002) Intelligent Systems in Biomedicine. In *Advances in Computational Intelligence and Learning* (pp. 437-460), Dordrecht, Springer.